

- A. R. Ubbelohde, *J. Chem. Soc.*, 1961 (1951).
39. Melaven, R. M., and Edward Mack, Jr., *J. Am. Chem. Soc.*, **54**, 892 (1932).
  40. Nasini, A. G., *Proc. Roy. Soc. (London)*, **A123**, 692 (1929).
  41. ———, and C. Rossi, *Gazz. chim. ital.*, **58**, 433 (1928).
  42. Phillips, P., *Proc. Roy. Soc. (London)*, **87**, 48 (1912).
  43. Rankine, A. O., *ibid.*, **A83**, 516 (1910).
  44. *Ibid.*, **88**, 575 (1913).
  45. Rankine, A. O., and C. J. Smith, *Phil. Mag.*, **42**, 615 (1921).
  46. Rappenecker, K., *Z. physik. Chem.*, **72**, 695 (1910).
  47. Rietveld, A. O., and A. van Itterbeek, *Physica*, **22**, 785 (1956).
  48. Sage, B. H., W. D. Yale, and W. N. Lacey, *Ind. Eng. Chem.*, **31**, 223 (1939).
  49. Schultze, Hugo, *Ann. Physik*, **5**, 140 (1901).
  50. Shimotake, Hiroshi, and George Thodos, *A.I.Ch.E. Journal*, **4**, 257 (1958).
  51. Smith, A. S., and G. G. Brown, *Ind. Eng. Chem.*, **35**, 705 (1943).
  52. Sperry, E. H., and Edward Mack, Jr., *J. Am. Chem. Soc.*, **54**, 904 (1932).
  53. Suhrmann, Rudolph, *Z. Physik*, **14**, 56 (1923).
  54. Sutherland, B. P., and Otto Maass, *Can. J. Res.*, **6**, 488 (1932).
  55. Sutherland, W., *Phil. Mag.*, **36**, 507 (1893).
  56. Titani, Toshizo, *Bull. Chem. Soc. Japan*, **5**, 98 (1930).
  57. *Ibid.*, **7-8**, 255 (1933).
  58. Trautz, Max, and P. B. Baumann, *Ann. Physik*, **2**, No. 5, p. 733 (1929).
  59. Trautz, Max, and Robert Heberling, *ibid.*, **10**, No. 5, p. 155 (1931).
  60. *Ibid.*, **20**, 118 (1934).
  61. Trautz, Max, and I. Hussein, *Ann. Physik*, **20**, 121 (1934).
  62. Trautz, Max, and Friedrich Kurz, *ibid.*, **9**, No. 5, p. 981 (1931).
  63. Trautz, Max, and Walter Ludewigs, *ibid.*, **1**, 409 (1930).
  64. Trautz, Max, and A. Melster, *ibid.*, **7**, No. 5, p. 409 (1930).
  65. Trautz, Max, and Fritz Ruf, *ibid.*, **20**, No. 5, p. 127 (1934).
  66. Trautz, Max, and K. G. Sorg, *ibid.*, **10**, 81 (1931).
  67. Trautz, Max, and F. W. Stauf, *ibid.*, **2**, No. 5, p. 737 (1929).
  68. Trautz, Max, and Walter Weizel, *ibid.*, **78**, 305 (1925).
  69. Trautz, Max, and Helmut Zimmerman, *ibid.*, **22**, 189 (1935).
  70. Trautz, Max, and Robert Zink, *ibid.*, **7**, No. 5, p. 427 (1930).
  71. Uehling, E. A., and E. J. Hellund, *Phys. Rev.*, **54**, 479 (1938).
  72. Van Cleave, A. B., and Otto Maass, *Can. J. Res.*, **13B**, 140 (1935).
  73. Vasilescu, Virgile, Doctoral thesis, Univ. Paris, France (1940).
  74. ———, *Ann. Physik*, **20**, No. 6, p. 292 (1945).
  75. Vogel, Hans, *ibid.*, **43**, 1235 (1914).
  76. Wobser, R., and F. Müller, *Kolloid-Beih.*, **52**, 165 (1941).
  77. Yen, Kia-lok, *Phil. Mag.*, **38**, 582 (1919).

Manuscript received July 22, 1960; revision received November 7, 1960; paper accepted November 9, 1960. Paper presented at A.I.Ch.E. Cleveland meeting.

# The Drag Coefficients of Single Spheres Moving in Steady and Accelerated Motion in a Turbulent Fluid

L. B. TOROBIN and W. H. GAUVIN

Pulp and Paper Research Institute of Canada and McGill University, Montreal, Quebec, Canada

Drag coefficients of aerodynamically smooth spheres having a density variation of from 0.252 to 1.91 g./cc. and a diameter variation from 1.56 to 3.21 mm. were obtained for acceleration rates varying from 103.5 ft./sec.<sup>2</sup> to -30 ft./sec.<sup>2</sup> and for relative intensities of up to 45%. The particle-to-Eulerian macroscale ratios varied from 0.50 to 0.16, and the diameter-to-Eulerian microscale ratios varied from 10 to 2.

The drag coefficients were found to be a function of the particle Reynolds number and of the relative intensity but not of the acceleration and relative macro-and-microscale variations.

A transition theory for the system investigated is presented, which predicts that the product of the critical Reynolds number and the square of the relative intensity should be a constant; it is supported by the experimental results obtained.

The theoretical analysis of the momentum transfer occurring in multiparticle dilute phase solids-gas flow systems has been hindered by an inability to estimate the fluid drag forces which act on the individual particles owing to their movement relative to the fluid. The fluid drag force is related to the relative motion by the use of a coefficient of drag defined by

$$R = (1/2)C_D A_p \rho_o U_R^2 \quad (1)$$

Reliable drag coefficients have been evaluated only for bodies in steady motion with respect to turbulent-free flows, and these conditions are not encountered in most solids-gas systems. The drag coefficients indirectly obtained from pressure-drop data (1, 2, 3) are invalidated by the assumptions

made in their calculation. More direct methods in which the velocities of individual particles have been measured (4, 5, 6, 7, 8, 9) suffer in that the fluid velocity and turbulence parameters along the particle trajectory were not determined.

To completely characterize a momentum transfer situation in a turbulent fluid the turbulent parameters

L. B. Torobin is with Esso Research and Engineering Company, Linden, New Jersey.

must be measured since the free-stream vorticity can, under the proper conditions, precipitate profound changes in the particle boundary layer and wake structure which have a marked effect on the momentum transfer. The effects of free-stream turbulence are of greater importance in systems where the particles are moving concurrently with the stream than if they remain stationary. As an illustration consider an entrained particle moving at 90 ft./sec. in a fluid which has a mean velocity of 100 ft./sec. and a 5% intensity of turbulence. Since the particle boundary layer and wake are generated by a relative velocity of 10 ft./sec., they are subjected to a relative intensity of 50%. Ahlborn (10) has shown that high intensities can cause transition at particle Reynolds numbers as low as 40.

Whether or not the particle momentum transfer will be affected by the free-stream turbulence depends in a large measure on the stability of the attached and separated boundary layers and the possible alterations in the vorticity transfer rates in the particle wake. A discussion of the aerodynamic phenomena occurring in solids-gas flow systems has been presented elsewhere (11, 12, 13, 14, 15), and this section describes the experimental determination of the drag coefficients of single spheres moving concurrently with a turbulent fluid.

## THEORETICAL CONSIDERATIONS

In a laminar free stream a characteristic sharp reduction in the sphere drag coefficient from approximately 0.5 to 0.1 is the outward indication that the attached laminar boundary layer has developed an instability which has somehow progressed to a laminar-turbulent transition. The supporting evidence for various transition theories previously discussed (15) indicated that at relative intensities of less than 0.2% an inherent instability in the flow develops in the form of progressively amplified oscillations within a narrow frequency range. The frequency range is dictated by the boundary layer Reynolds number, and the dependency has been successfully predicted by the Tollmien-Schlichting theory (16). As the free-stream turbulence increases, it causes the adjacent frequencies to draw energy away at an ever increasing rate from the preferred frequency band (17). At a sufficiently high level the laminar oscillations would not play any part in the transition, and here the Taylor transition theory (18) would seem to be applicable.

Taylor assumed that transition was brought about by an instantaneous separation and reattachment of the

boundary layer due to the free-stream pressure fluctuations  $\partial p'/\partial x$  associated with the turbulent motion. These fluctuations are a function of the intensity  $\sqrt{u'^2}$  and the microscale  $\lambda$ . In isotropic turbulence the relationship is given by

$$\lambda/(L)^{1/2} = [B\nu/(\overline{u'^2})^{1/2}]^{1/3} \quad (2)$$

By incorporating some rather drastic assumptions, Taylor showed that the critical Reynolds number for transition depended on the following functional relationship:

$$(N_{Re})_c = \Phi(B)(\sqrt{\overline{u'^2}}/U_\infty)(d/L)^{1/5} \quad (3)$$

In addition the critical Reynolds number will be affected by departures from isotropy.

The Taylor parameter defined in Equation (3) has proven successful in correlating results obtained with fixed flat plates, elliptic cylinders, and spheres for turbulence levels of up to approximately 5%. Studies of the effect of higher levels of turbulence on the drag of fixed spheres have not been made, mainly owing to the difficulty of generating and measuring intensities in excess of 10%. At high relative intensities it may not be proper to consider the incident turbulent energy merely as a disturbance to an established laminar flow. Actually the particle surface is expected to create a laminar regime in the midst of a turbulent environment, and the question is really one of turbulent laminar transition.

The present authors would like to suggest an alternative transition criterion for high turbulent levels. It may be helpful to cite several characteristics of the system considered. The turbulent flow in a duct is in a state of dynamic equilibrium in which there is a production, diffusion, and dissipation of turbulent energies. A spherical particle entering this system may, by virtue of its relative motion and the viscous damping forces which are produced at its surface interface, create an isolated region of quasilaminar flow in its immediate vicinity as a laminar boundary layer and wake. Throughout its entire length this fluid system will be subjected to the disturbances from the free-stream turbulence. The nature of the disturbances may be such that they would soon die out if introduced only at a given region of the boundary layer, but since they occur over the complete surface of the sphere system, their effect will be governed by the extent and depth to which they can penetrate the laminar flow.

A volume element upstream from the sphere which, by definition, eventually becomes part of the laminar motion on the sphere must have all of its

turbulent energy dissipated by the viscous damping forces in the sphere environment before it enters the laminar flow. The turbulent energy of the incident fluid element will be given in Cartesian tensor notation by

$$E_t = (1/2)\rho_0 \iiint dx_1 dx_2 dx_3 \overline{u'_i u'_i} \quad (4)$$

and the depth within the boundary layer to which the volume element will penetrate before losing all of its turbulent energy will be a function of  $E_t$ .  $E_t$  in turn will be a function  $\Phi_1$  of  $(\rho_0 \overline{u'^2})$  per unit volume. The distance penetrated will also be a function of the viscous damping forces set up by the velocity gradients at the sphere surface. Viscous damping forces per unit volume may be expected to follow the functional relationship

$$F_v = \Phi_2 \mu \partial(\partial U_1/\partial x_2)/\partial x_2 \quad (5)$$

$$F_v \approx \Phi_3 \mu \overline{U_1}/x_2^2 \quad (6)$$

If it is further assumed that the characteristic length over which the damping forces act is a function of the sphere diameter, then the viscous damping energy associated with the damping action will be

$$E_v = \Phi_4 \mu \overline{U_1}/d \quad (7)$$

The ratio  $E_t/E_v$  will therefore specify the extent of penetration of the turbulent energy with respect to the sphere surface, and it will be given by

$$E_t/E_v = \Phi_5 \left( \frac{\rho_0 \overline{u'^2} d}{\mu \overline{U_1}} \right) \left( \frac{\overline{U_1}}{\overline{U_1}} \right) \quad (8)$$

$$= \Phi_5 (N_{Re}) \left( \frac{\sqrt{\overline{u'^2}}}{\overline{U_1}} \right)^2 \quad (9)$$

If a disturbance penetrates to the sphere surface, Lin (19) has shown that viscosity effects acting at the wall will lead to a phase shift between its axial velocity component  $u'_1$  and its normal velocity component  $u'_2$  so that the turbulent shear stress  $(-\rho_0 \overline{u'_1 u'_2})$  will have a positive value. Hinze (20) points out that since  $(\partial \overline{U_1}/\partial x_2)$  at the wall must be greater than zero, the turbulence production term  $-(\partial \overline{U_1}/\partial x_2)(\rho_0 \overline{u'_1 u'_2})$  will be positive and there will be a generation of turbulence in the boundary layer-flow. Hinze feels that this analytic result is supported by the experimental conclusions reached by Lindgren (21) who found that at transition "... turbulence should originate from wall effects acting on disturbed flow in the immediate vicinity of—or in contact with—the boundary walls."

The present authors suggest that at transition  $(E_t/E_v)$  will have reached a critical value  $(E_t/E_v)_c$  which will

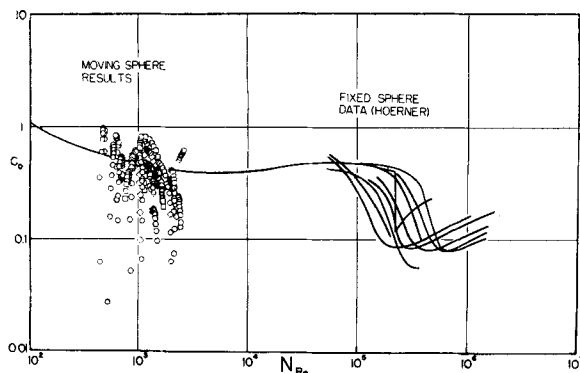


Fig. 1. Drag coefficient for spheres moving in a turbulent flow.

allow sufficient penetration for the production of turbulence in the boundary-layer flow. If this is correct, then at transition

$$(E_t/E_v)_c = \Phi_b(N_{Re})_c (\sqrt{u'^2_1}/U_1)^2 \quad (10)$$

so that (when one reverts to the original notation)

$$(N_{Re})_c (\sqrt{u'^2}/U_R)^2 = \text{constant} \quad (11)$$

## EXPERIMENTAL

A novel particle ballistics wind tunnel and radiotracer particle velocity measurement technique was developed to allow the quantitative determination of the drag coefficients of single particles moving in both steady and accelerated motion. A detailed description of the apparatus and procedures has been given previously (22). In essence the radioactive test particles were launched in a nonrotating manner along the axis of an 8-in. vertical turbulent flow wind tunnel with an 18-ft. test section which was calibrated for the mean velocity and turbulence parameters. Continuous and precise records of the particle motion obtained with the tracer method were processed by an IBM-650 program, and the first, second, and third derivatives of the motion, as well as the instantaneous drag coefficients and particle relative intensities, were calculated.

The test particles used were aerodynamically smooth spheres having a density variation of from 0.252 to 1.91 g./cc. and a diameter variation of from 1.56 to 3.21 mm.

## RESULTS

Experimental data and calculated results for thirty-two runs are summarized in Table 1.\* Shown in this table are time, distance, instantaneous velocity, acceleration, rate of change of acceleration, particle Reynolds number, drag coefficient, and relative intensity.

\* Tables of data and results have been deposited as document No. 6888 with the American Documentation Institute, Photoduplication Service, Library of Congress, Washington 25, D. C., and may be obtained for \$5.00 for photoprints or \$2.25 for 35-mm. microfilm.

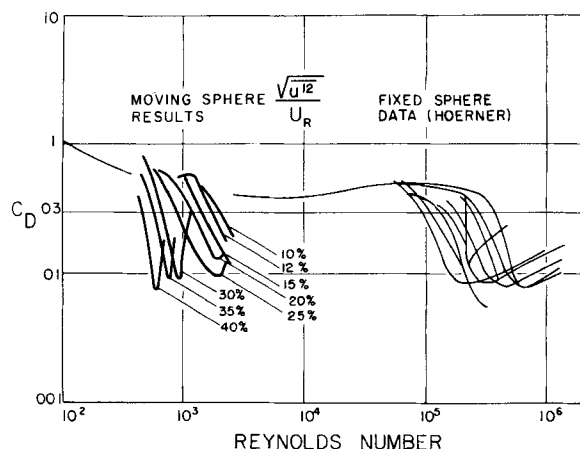


Fig. 2. The effect of the relative intensity on the drag coefficients of spheres.

Figure 1 shows the drag coefficients which were obtained, plotted as a function of the particle Reynolds number. Many of the results are not observed on the plot because of the superposition of values, particularly in the region of the standard drag curve. In a firing sequence the entrance velocity was gradually increased, and this resulted in a preponderance of data in the regions removed from criticality.

Constant relative intensity curves were drawn through the results by interpolation, and these are shown in Figure 2. The results for lower but unspecified intensities given by Hoerner (23) are also reproduced to show the similarity in the curve structure. Fortunately the particle Reynolds number change during each firing was small in comparison with the intensity differences caused by the axial gradient of the intensity in the test section, so that the occurrence of transition was clearly marked by a sharp progressive drop or increase in the drag coefficient during a flight.  $(N_{Re})_c$  is by convention the Reynolds number at which the steeply-sloped section of the constant intensity curve intersects the drag value of 0.3. Values of  $(N_{Re})_c$  for different intensities are shown in Figure 3. The experimental drag values rather than the intersections of the mean curves were used, and the data lie on a smooth curve. Drag values of 0.3 can occur at Reynolds numbers other than  $(N_{Re})_c$ , but the change of  $C_D$  with changing intensities would be a very gradual one. The  $C_D$  values of 0.3 which were not clearly associated with a transition phase were not included in the plot.

The intensity profiles towards the end of the test section tended towards the profiles obtained in fully developed pipe flow, so that they became progressively sharper. In this region the possible error in estimating the relative intensity becomes unacceptably large, since there is an appreciable intensity

gradient across the constant velocity 2-in. core. Departures from the axis of the order of 1/2 in. could probably escape detection on the pulse pattern, and yet the intensity error would be significant. In one case a slight velocity inversion was recorded with a particle having a normal pulse pattern, whereas the adjacent firings were normal, and this was probably due to a sharp intensity increase. In order to minimize the possible error, values beyond the 14-ft. level were not included in the relative intensity curves.

## DISCUSSION OF RESULTS

The particle velocity histories obtained formed smooth curves, although the method of calculation did not exert a smoothing influence. As the firing pressure was increased, the particle velocity histories for a given sphere showed a decreasing convergence to a quasi steady state value for the turbulence conditions prevailing at the end of the test section. When the test spheres were fired in above this value, they gradually decelerated towards the equilibrium velocity with a deceleration less than gravity. Superimposition of the pulse patterns of adjacent firings showed that there was much duplication, so that in general only every second film was analyzed.

Data obtained with accelerating and decelerating particles covering a range of 103.5 ft./sec.<sup>2</sup> to -30 ft./sec.<sup>2</sup> yielded approximately the same drag coefficients for similar conditions, and the results seemed to be unaffected by their position in the column, that is the time elapsed from the initiation of their motion. This contradicts the acceleration behaviour noted by Lunnion (24) in a laminar stream for the same Reynolds number region and for acceleration less than 32 ft./sec.<sup>2</sup> which was discussed in reference 13. It will be recalled that studies in laminar fluids

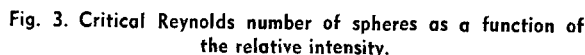
Figure 4 shows the results obtained, each point being obtained from different firings but at a constant intensity of 10.0%. Even though the sampling time was extremely short (the entire flight through the test section taking less than 0.2 sec.) and the process variables were changing continuously, the scatter is considerably less than is usually obtained in the transition region. The standard drag coefficient curve and the curves obtained by Lunnon (24) for accelerations of 0 and 25.6 ft./sec.<sup>2</sup> are also shown. Lunnon's data are the most accurate obtained as yet for a sphere falling in quiescent

As discussed in reference 15 heat transfer studies provide the only comparisons with systems having similar Reynolds numbers and intensities, and it will be recalled that the results given for spheres showed no explicit scale dependency. In the case of cylinders the results in some cases showed no scale dependency, whereas the averaged curves obtained by van der Hegge Zijnen (25) clearly indicate a scale dependency having a trend in the opposite direction, contrary to that predicted by the Taylor theory.

It appears from the results obtained that at low relative intensities the drag coefficients do not differ appreciably from those found previously for laminar fluids. In other words the standard drag curve values can safely be used at low relative intensities of turbulence. As the intensities increase, there is a gradual and moderate increase in the momentum transfer. This trend, which has also been noted in other drag investigations at low intensities, again suggests that the turbulence has affected the vorticity transfer in the wake alone. A further intensity increase causes the drag curve to drop gradually at first and then sharply to a minimum, and this behavior must result from a transition to a new regime in the flow structure surrounding the sphere. Further increases in intensity cause an upswing in the curve to values which, in the case of high intensities, approach the standard curve. This behavior is very similar to the transition curves due to surface roughness and fluid turbulence shown in Figures 1 and 2. In the case of extreme roughness it was found that the

The sharp minima are interesting. Although similar trends have appeared in some of the curves reported at higher Reynolds numbers with supported spheres in turbulent wind-tunnel flow, it may be that this phenomenon occurs more readily with freely moving bodies and as such would offer an explanation for the remarkably low drag values found at low Reynolds numbers by Fledderman and Hanson (8) and others. Transition processes are not well fixed in that the behavior must be integrated over a sufficient period of time to obtain a constant average. In the case of a moving particle the free-stream vorticity may cause a metastable state of motion to occur which would not be sustained for an indefinite period of time or with the presence of a disturbing support mechanism. Furthermore the wake shedding process is different for restrained and freely moving bodies, and even with restrained bodies Wiselius (26) has found that changing the tightening loads used to restrain the sphere will cause significant alterations to the drag coefficient in the critical region.

Lunnon's accurate results and those obtained more recently by Barker (27) have shown that the drag coefficients for freely moving spheres in still air differ from those obtained with fixed bodies for the post-Stokesian Reynolds number range. A further drag coefficient variation must occur with particles moving in a turbulent flow as the particle diameter becomes lower than the macroscale. If the motion is observed in a sufficiently short time interval, the intensity to which the particle system is being subjected will not be equal to the mean measured R.M.S. value but will depart from it increasingly in a random manner as the sampling time is reduced. This effect will be considerably amplified in the critical region.



The ballistics wind-tunnel results show that with decreasing Reynolds numbers the sphere fluid system becomes increasingly immune to the incident turbulence. The values of  $(N_{Re})_c$  when plotted against their corresponding relative intensities formed a smooth curve having a near parabolic shape. In accordance with the theory proposed by the authors the product of the critical Reynolds number and the square of the intensity should be a constant for a given system. In Figure 3 the equation

$$(N_{Re})_c (\sqrt{u'^2}/U_R)^2 = 45 \quad (12)$$

has been superimposed on the experimental data, and in view of the assumptions made and the expected scatter in results the agreement is surprisingly good. At the low Reynolds number values the theoretical curve indicates a lower intensity than was found experimentally, but this would be expected since the definition of  $(N_{Re})_c$  used in the plot (that is the value at which a transition curve intersects the  $C_D = 0.3$  line) does not correspond to the one used in the theory in that the former is not directly linked to the onset of turbulent motion.

As the Reynolds numbers decrease, transition must occur at a higher drag coefficient, particularly where the skin friction component of the drag becomes significant. The length of the transition zone as well as the separation angle in the Reynolds number region investigated in this work must be different from those at high Reynolds numbers where the convention  $C_D = 0.3$  served as a good approximation to the actual transition Reynolds number. A laminar-turbulent transition in the attached boundary layer causes a decreased drag by decreasing the angle made by the separation ring with the rear stagnation point. Available experimental evidence indicates that the sphere wake in the Reynolds number range investigated differs from the wake in the vicinity of  $10^5$ , and the alterations that the former undergoes as a result of the free-stream turbulence may be unlike the changes produced in the latter. There is a possibility therefore that the similarity of the intensity curves obtained to those found previously at lower intensities is somewhat misleading.

## CONCLUSIONS

Increasing free-stream vorticity relative to the motion generating the particle boundary layer and wake will at first cause a moderate increase and then a sharp decrease of the particle drag coefficient. The increase corresponds to a disruption of the wake

system, while the sharp decrease is due to a laminar-turbulent transition in the attached boundary layer in a manner analogous to the well-known behavior at higher Reynolds numbers.

A further indication of a disruption of the particle wake is the lack of the acceleration effects noted in laminar fluids.

The variation of the critical Reynolds number with the turbulence intensity would seem to confirm a transition theory proposed by the authors for momentum transfer at high intensi-

ties which predicts that  $(N_{Re})_c \left( \frac{\sqrt{u'^2}}{U_R} \right)^2$

should be constant for a given system.

For the diameter-to-scale ratios employed no turbulence scale effect was evident.

## ACKNOWLEDGMENT

The authors wish to express their appreciation to Mr. E. K. Marchildon for his assistance with some of the measurements. L. B. Torobin is indebted to the Scientific Research Bureau, Trade and Commerce Department, Province of Quebec, for three consecutive fellowships in support of his research program.

## NOTATION

Any consistent set of units may be employed. Those listed are merely illustrative.

- $A_p$  = particle cross-sectional area, sq.ft.
- $B$  = constant in Equation (2), dimensionless
- $C_D$  = coefficient of drag, dimensionless
- $d$  = particle diameter, ft.
- $E_t$  = turbulent energy, ft.-poundals/cu.ft.; total turbulent energy in Equation (4), ft.-poundals
- $E_v$  = viscous damping energy, ft.-poundals/cu.ft.
- $F_v$  = viscous damping force, poundals/cu.ft.
- $L$  = Eulerian macroscale of turbulence, ft.
- $p$  = free-stream pressure, lb. force/sq.ft.
- $R$  = drag force, poundals
- $(N_{Re})_c$  = critical Reynolds number for transition, dimensionless
- $u'$  = velocity fluctuation of fluid in  $x$  direction, ft./sec.
- $\ddot{U}$  = particle acceleration, ft./sec.<sup>2</sup>
- $\bar{U}$  = mean fluid velocity, ft./sec.
- $U_R$  = particle velocity relative to fluid, ft./sec.
- $x$  = length scale in direction of mean flow, ft.;  $x_1, x_2, x_3$  = Eulerian Cartesian coordinates in tensor notation

## Greek Letters

- $\lambda$  = Eulerian microscale of turbulence, ft.

- $\mu$  = fluid viscosity, lb./ft. (sec.)
- $\nu$  = fluid kinematic viscosity, sq. ft./sec.
- $\rho_u$  = fluid density, lb./cu.ft.
- $\Phi$  = functional relationship,  $\Phi_1, \Phi_2, \Phi_3, \Phi_4, \Phi_5$  [Equations (5) to (10)] are constants

## Subscript

- $i$  = index of tensor, which can take the values 1, 2, and 3 to indicate each of the coordinates. If index is repeated [as in Equation (4)], summation should be made over these three values

## LITERATURE CITED

1. Focking, N. L., Ph.D. thesis, Cornell Univ., Ithaca, New York (1951).
2. Mehta, N. G., Ph.D. thesis, Purdue Univ., Lafayette, Indiana (1955).
3. Mitlin, A., Ph.D. thesis, Univ. London, England (1954).
4. Ingebo, R. D., *Natl. Advisory Comm. Aeronaut. Tech. Note* 3762 (1956).
5. Manning, W. P., and W. H. Gauvin, *A.I.Ch.E. Journal*, **6**, 184 (1960).
6. Pasternak, I. S., and W. H. Gauvin, *ibid.*, **7**, 254 (1961).
7. Khudiakow, G. N., *Izv. Akad. Nauk. S.S.S.R. Otdel. Tekh. Nauk.*, **7**, 1022 (1953).
8. Fledderman, R. G., and A. R. Hanson, *U. Mich. Eng. Res. Inst. Rep. No. CM 667* (1951).
9. Chernov, A. P., *Izv. Akad. Nauk. Kaz. S.S.S.R., Ser. Energ.*, **9**, 160 (1955).
10. Ahlborn, F., *Zt. Fur Technische Physik.*, **12**, 10 (1931).
11. Torobin, L. B., and W. H. Gauvin, *Can. J. Chem. Eng.*, **37**, 129 (1959).
12. *Ibid.*, p. 167.
13. *Ibid.*, p. 224.
14. *Ibid.*, **38**, 142 (1960).
15. *Ibid.*, p. 189.
16. Schlichting, Herman, *Nachr. Ges. Wiss. Gottingen, Math. Phys. Klasse*, p. 181 (1933).
17. Bennett, H. W., and C. A. Lee, *Proc. Am. Soc. Civ. Engrs.*, **81**, 796 (1955).
18. Taylor, G. I., *Proc. Roy. Soc.*, **156A**, 307 (1936).
19. Lin, C. C., *Proc. Nat. Acad. Sci.*, **40**, 741 (1954).
20. Hinze, J. O., "Turbulence," McGraw-Hill, New York (1959).
21. Lindgren, E. R., *Arkiv Fysik*, **12**, 1 (1957).
22. Torobin, L. B., and W. H. Gauvin, *A.I.Ch.E. Journal*, **7**, No. 3, p. 406 (1961).
23. Hoerner, S., *Luftfahrtforschung*, **12**, 42 (1935).
24. Lunnun, R. G., *Proc. Roy. Soc.*, **110A**, 302 (1926).
25. van der Hegge Zijnen, B. G., *Appl. Sci. Res.*, **A7**, 205 (1958).
26. Wiseluis, S. I., *Netherland Aeronaut. Res. Inst. Rep. A 950*, Amsterdam (1947).
27. Barker, D. H., Ph.D. thesis, Univ. Utah, Salt Lake City, Utah (1951).

Manuscript received August 2, 1960; revision received February 10, 1961; paper accepted February 15, 1961. Paper presented at A.I.Ch.E. San Francisco meeting.